DOI: 10.2507/29th.daaam.proceedings.072

AERODYNAMIC STUDY OF THE ENVIRONMENTAL VEHICLE MODEL WITH THE FLOW SIMULATION CFD PROGRAM

Krasimir Tuzharov, Simeon Iliev & Dancho Gunev

This Publication has to be referred as: Tuzharov, K[rasimir]; Iliev, S[imeon] & Gunev, D[ancho] (2018). Aerodynamic Study of the Environmental Vehicle Model with the Flow Simulation CFD Program, Proceedings of the 29th DAAAM International Symposium, pp.0495-0504, B. Katalinic (Ed.), Published by DAAAM International, ISBN 978-3-902734-20-4, ISSN 1726-9679, Vienna, Austria
DOI: 10.2507/29th.daaam.proceedings.072

Abstract

With this study, the design and performance of the vehicle's body may be improved by analysing the factors that affect the aerodynamics. The challenge of this study is to be able to design and to construct a vehicle body that will have less drag than commercial vehicles in accordance with the existing competition rules to help achieve better energy efficiency. Modern CAE methods provide high capabilities for optimized designs and fast design processes. The practical use of these processes is shown by an example of an efficient vehicle for the Shell Eco-marathon. The work produces CFD modelling of the aerodynamic characteristics of the electrical vehicle model and is compared with the characteristics of similar models obtained from other authors. The aerodynamic characteristics of the Team Avtomobilist's vehicle are, better. At vehicle speed $v = 10\ m/s$, the smallest value of the drag coefficient of the vehicles involved in the race is $C_x = 0{,}085$, whereas the one of the Team Avtomobilist is $C_x = 0{,}065$, i.e. with 25% smaller.

Keywords: CFD Simulation; vehicle aerodynamics; electric vehicle; vehicle body

1. Introduction

In the stages of its development, the vehicle has been subjected to various factors influencing its appearance. Reducing oil resources and rising prices cause serious measures on the part of designers to increase fuel economy. Until the 1980s, only part of the models produced had an appropriate body shape specifically designed to reduce air drag force [1], [2].

In the beginning, the research is mainly done on aerodynamic drag reduction. It is very clear that the stability of the vehicle depends not only on the air flow below it, but also on the side impact of the wind. Complex experiments and computational methods are needed to determine the effect of aerodynamic forces on vehicle movement. Recently, the new research tool, Computational Fluid Mechanics (CFD), has been used for their research. In this approach, the flow area is calculated by means of different forms of the Nave-Stocks' private differential equations, including closing turbulent equations known as turbulent models, which differentiate the system into a solvable state. The fluid area (computing area) is divided into multiple volumes (cells) for each of which the flow parameters are calculated. This method does not make too many simplifying prerequisites. The question arises, what is the accuracy of the decision?

In conjunction with these facts arose the idea of creating Shell Eco Marathon competition, which promoted highly efficient vehicles. One of these vehicles was created in the student scientific team "Avtomobilist" that one in 2018 took 9th place passing 472km/kWh. In order to improve this results, it was decided to identify aerodynamic characteristics of the vehicle and to change the line of its shape. From the beginning, it was looked for and raised the collaboration with small business located in an area close to the University of Ruse to help in the manufacturing process of the prototypes and to allow the students to have the experience of working in a real production environment [3], [4].

2. Exposition

The object of the study is an electric vehicle model (Fig. 1), which participates in the international competition Shell Eco- Marathon 2018. The dimensions of the model are: length l = 2680 mm, height h = 630 mm and width w = 670 mm. The air flow flows through the vehicle, whereby the speed and the pressure are distributed on the surface of the vehicle so that an aerodynamic resistance force R is created, which decomposes into two components - the force of the drag X, which is parallel to the inertial current and the lifting force Y, which is perpendicular to the inertial flow. In order to simulate the flow between the vehicle and the ground, the model 1 of the electric vehicle is placed on the plate 2.

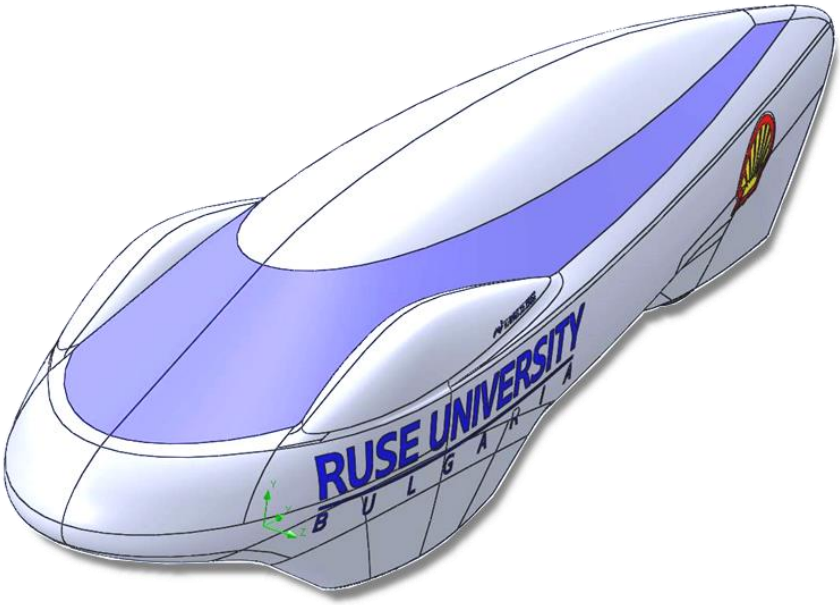

Fig. 1. Model of the electric vehicle

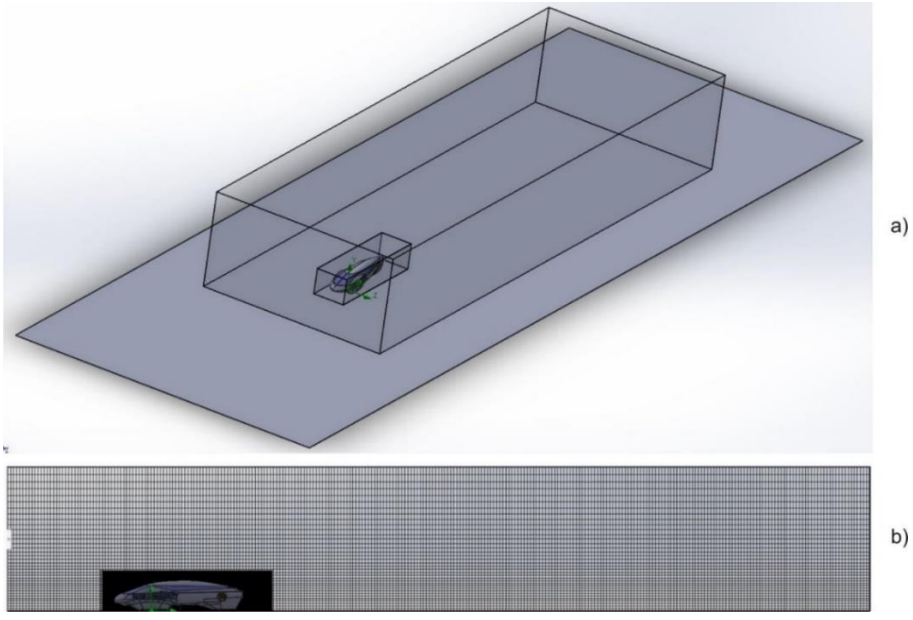

Fig. 2. Calculation model and computing network in the XY plane

The aim of the report is to obtain the aerodynamic characteristics of the electric vehicle, which are dependences of the coefficients of the aerodynamic forces at different constant air velocities v=2,4,6,8,10 m/s, which are presented in a dimensionless form as the number of Reynolds Re. In order to achieve the goal, the following tasks have been solved: a physical model of the electric vehicle with the Solid Works program, and a numerical model (Figure 2a) with the CFD program Flo Simulation were created using the Wizard option. The vehicle's model is placed on a plane that simulates the ground. The type of analysis is external, three-dimensional, the computing area before, after and side of the electric vehicle is extended to the auto-generated, in order to obtain convergence and higher accuracy of the solution. Its dimensions in meters are respectively on the x-axis: -3, +15; on the y-axis: 0, +3 and on the z-axis: -3, +3.

Prerequisites for the study are that the fluid is air, the flow is turbulent with a laminar sublayer at the walls of the electric mobile, the walls are heat-insulated (the flow is adiabatic). Taking into account that there are cavities in the geometric model, which have to be excluded from the pattern, the **Exclude cavities without flow conditions**.

The general project settings are shown in Table 1. The table shows that the default conditions are left by default by activating the Pressure potential option. In Flow Simulation, turbulent fluid flows are modelled with the Nave-Stokes equations [5], [6] that describe the laws of storage of matter, impulse and energy. Flow parameters are averaged over time, according to Reynolds. As a result, the equations have additional members - Reynolds tensions. To close the equation system in Flow Simulation, turbulence intensity I and turbulence length l are used within the turbulent model: turbulent intensity-turbulent length I-1 [5], [6].

Unit system	SI
Wall Conditions	Default smooth walls
Initial and Ambient Conditions	Thermodynamic parameters: Temperature 293°K; Pressure: 101325 Pa; Turbulence parameters: turbulence intencity 0,1 %, turbulence length 0,07 m.
Global set meshing	Type of meshing creation: automatic; Result resolution: 5; Ratio factor 1.

Table 1. The general project settings

The boundary conditions for the input of a computing area (Fig. 2) that is prism-shaped are: the velocity of the flow, the values of the pressure p=101325 Pa and the temperature T=273 K of the environment. The roughness of the walls is neglected.

To set up the initial mesh, the **Automatic settings** mode is disabled, and the number of the cells of the base mesh is determined by coordinates - for the axis x Nx = 300, for the y axis Ny = 35, for the z Nz = 100; it is assumed that the level of pre-crushing of the mesh near to the walls is 2 at a maximum of 9; the curvature criterion is 0,3 rad; the tolerance criterion of 0,0001 m; the other mesh refinement indexes are on the default of the program. The resulting base mesh in the XY plane is shown in (Fig. 2 b).

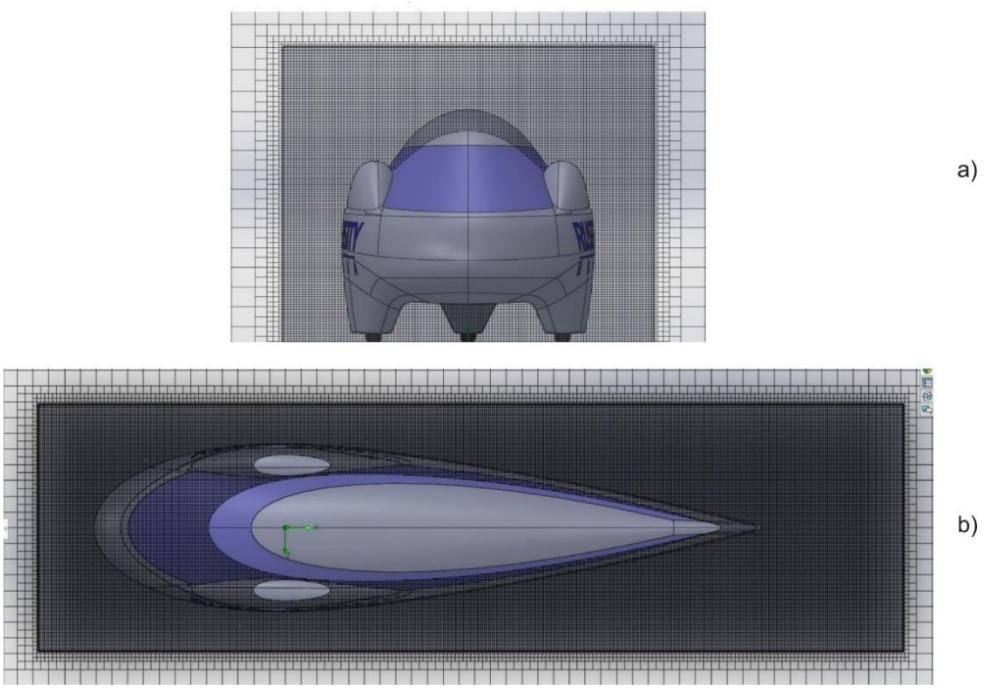

Fig. 3. Calculation networks for the x-y and z-y planes respectively

To optimize the network around the vehicle, a **Local Mesh** function has been used. A body has been created in advance that covers with reserve the vehicle (Fig. 2 b and Fig. 3) and is assigned the **Disable** attribute, which makes the body transparent to the flowing environment. The level of refining of fluid cells and those that are in contact with solid walls are increased 3 times in the **Refining Cells** option. The **Cannels** option is also enabled due to the flow between the floor of the vehicle and the ground. The number of cells across the channel is set to 10, and is raised to 2 for the maximum channel refining level with the Maximum Channel Refinement Level button.

The **Advanced Refinement Level** options are set to 2 for Small Solid Feature Refinement level and Curvature Level; 0.1 rad for Curvature Criterion; 0.001 m for Tolerance Criterion.

After the described settings, the local network is generated, which has been shown in (Fig. 3a and Fig. 3b). The transverse mesh between the base and the local is also visible in the figure.

As far as the result is concerned, the grid is sufficiently rational - the total number of cells from the fluid medium is 6 041100 and the partial cells between the rigid walls and the fluid medium 350 551 as the mesh thickens at the walls of the vehicle and the gap between the bottom of the vehicle the earth's surface. With the mesh so obtained, the task is convergence and the computing time is 18 hours.

After the described settings, the local mesh shown in (Fig. 3a and Fig. 3b) is generated. The transitional mesh between the base and the local is also visible in the figure.

As far as the result is concerned, the grid is sufficiently rational - the total number of cells from the fluid medium is 6 826 616 and the partial cells between the rigid walls and the fluid medium 184 612, as the mesh thickens at the walls of the vehicle and the gap between the bottom of the vehicle the earth's surface. With the grid so obtained, the task is convergence and the computing time is 18 hours.

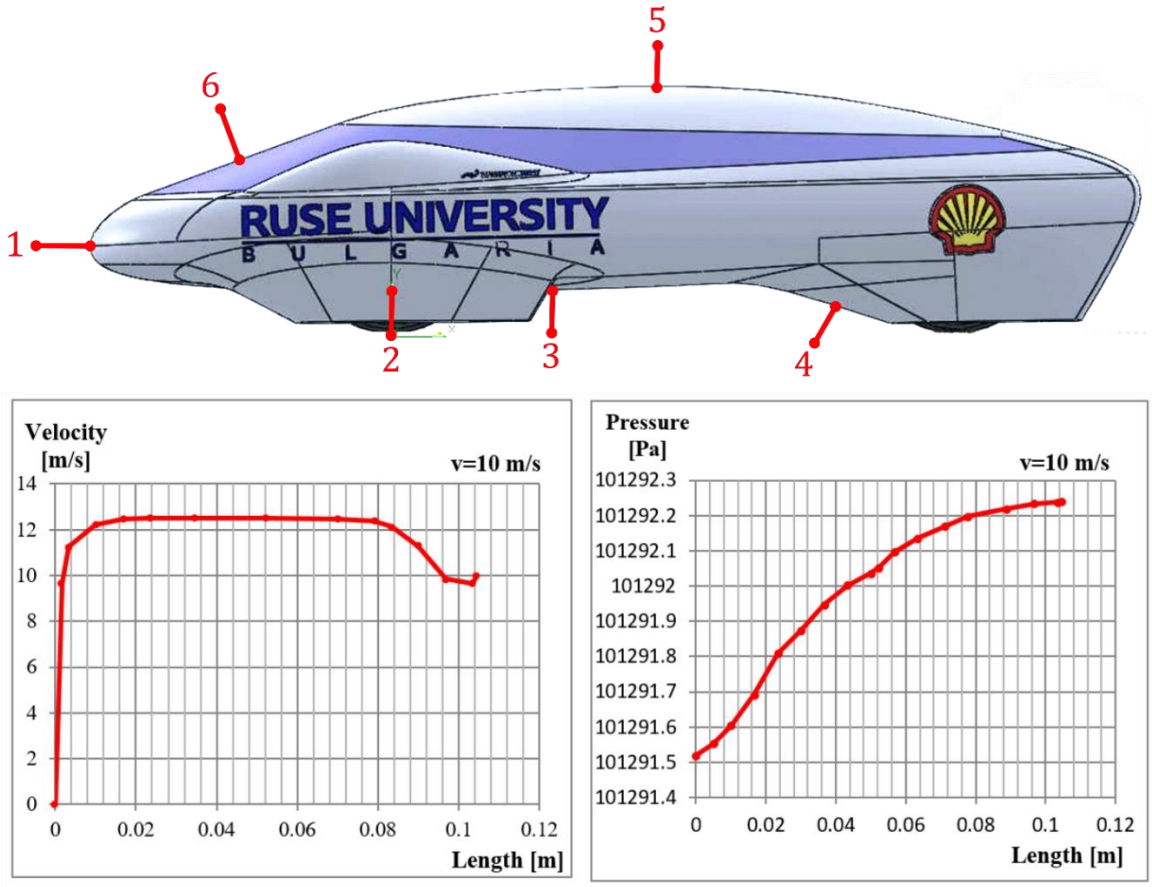

Fig. 4. Control lines around the vehicle and speed distribution along their length, to determine the thickness of the boundary layer

A way to compare the theoretical trends obtained by different methods with the experimental data is by comparing the results for control points, control lines or control loops. The (Fig. 4a) shows six control lines located in different sections around the vehicle. They are numbered 1 to 6 in the counter clockwise direction, counting starting from the line that comes out of the nose point of the vehicle.

The global objectives of the project are to determine the distribution of pressure and speed in the flow around the vehicle, the turbulent intensity and turbulent length resulting from the simulation. Surface objectives are the determination of aerodynamic forces in the direction of the X and Y axes, as and the intensity of the vortices on the surface of the vehicle.

The computational purposes are the calculation of the number of Re and the aerodynamic coefficients of the drag force - Cx and the lift force - Cy. The power of the engine that is spent to overcome the aerodynamic resistances is calculated too. The distribution of pressure and velocity in the flow is the result of the solution of the Reynolds-Nave-Stokes private differential equations. The values of the aerodynamic forces on the vehicle surface for various constant velocity values v of the non-disturb flow at a given pressure distribution are modelled by the built-in the program universal functions:

$$X = \int_S p(S), \;\; Y = \int_S p(S) \tag{1}$$

where S is the surface of the vehicle; $p(S)$ - the distribution of the pressure over the surface of the vehicle; X and Y - the values of aerodynamic forces.

The power to overcome aerodynamic resistances and the non-dimensional coefficients of the drag and lift forces are calculated by inserting dependencies with the option **Insert Equation Goals** respectively for power

$$P = Xv \tag{2}$$

for coefficient of drag force

$$C_X = \frac{2X}{\rho v^2 S} \tag{3}$$

for coefficient of lift force

$$C_Y = \frac{2Y}{\rho v^2 S} \tag{4}$$

where ρ is the density of the air.

3. Results and analysis

Overall, in the course of the decision, the task exhibits stability and rapid convergence especially for the power indicators - the aerodynamic forces, as well as for all the objectives of the project at the 10th iteration (Fig. 5a), the most are the iterations for determining the friction forces - 50 (Fig. 5b).

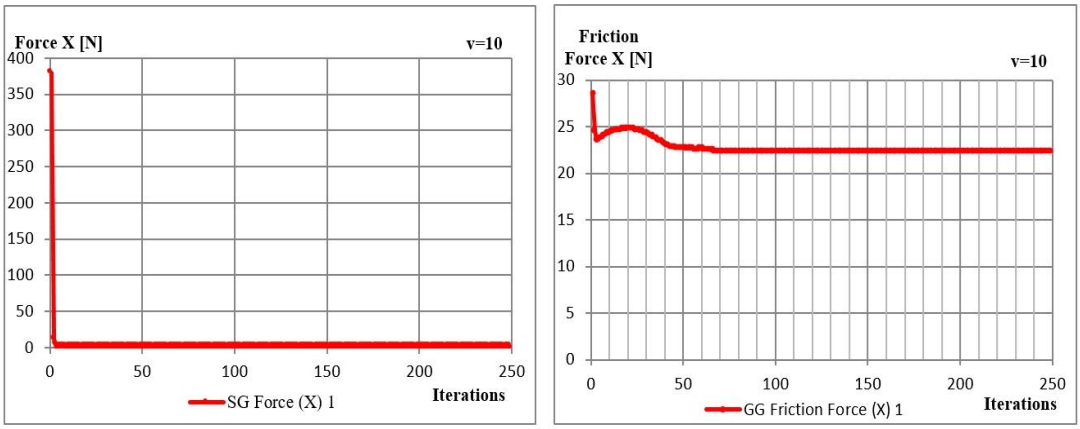

Fig. 5. The aerodynamic forces and friction forces.

As stated in the exposition with the Reynolds equation, the distribution of velocities and pressure around and on the surface of the vehicle are determined. The results for the speed field in the vertical, horizontal and transverse sections of the immersed vehicle at the speed $v = 10\ m/s$ of the undisturbed flow are shown in (Fig. 6) and (Fig. 7). It is seen that the vehicle in the vertical plane X-Y has the form of a double sided wedge, which is why it most strongly deforms the flow in the cross section passing through the front wheels (Figure 6a). In this section are located the isotahs with the highest speed - $v_i = 13\ m/s$. In the X-Z horizontal planes at different altitudes, the shape is like a drop profile and changes from the geometry of the fenders (Fig. 6b) and (Fig. 6c).The largest deformation of the flow is also in the area of the cross section passing through the front wheels.

Because of the symmetry of the vehicle, the isotahs are also symmetrical, as the shape also influences the shape of the fenders section with the plane (Fig. 7a). The isotachs with the highest speed and here are around $v_i = 13\ m/s$ too.

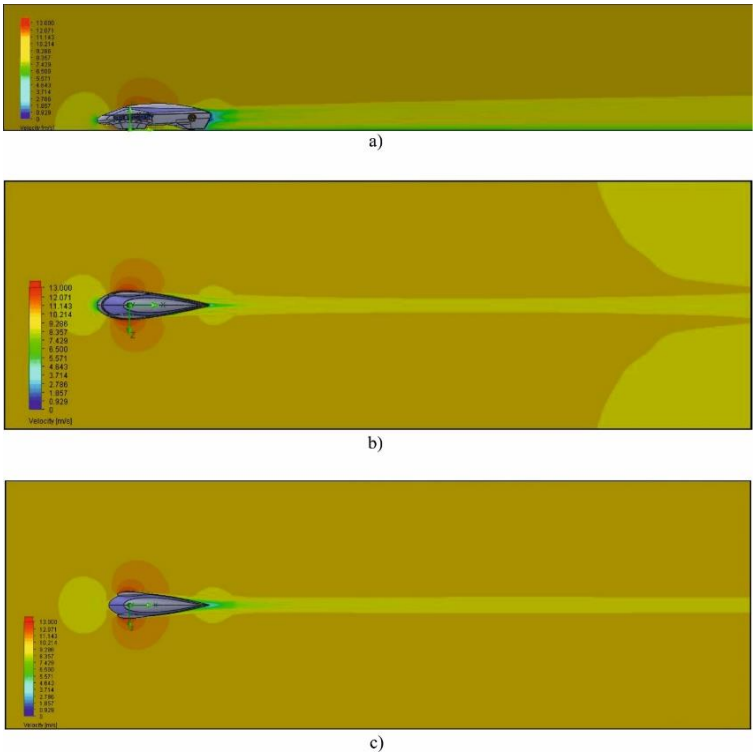

Fig. 6. The velocity field (isotachi) at the speed $v = 10\ m/s$ of the undisturbed flow in vertical and two horizontal sections The aerodynamic forces and friction forces

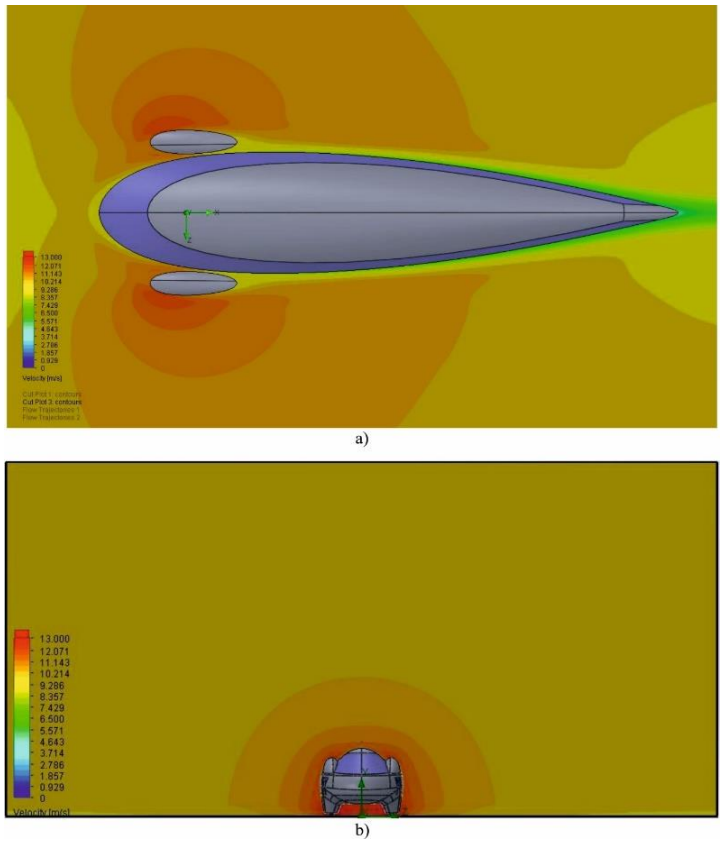

Fig. 7. The speed field (isotahs) at the speed $v = 10\ m/s$ of the undisturbed current in horizontal (close-up) and cross-sections

The speeds in front and after the vehicle are roughly the same - around $v_i = 6{,}5\ m/s$, that gives rise and pressure equalization. The picture is changed by changing the coordinate Y on the plane in which the current is shown (Fig. 6c) and (Fig. 7a). The backflow of the vehicle breaks away from the walls without swirling. These are prerequisites for low values of the drag force.

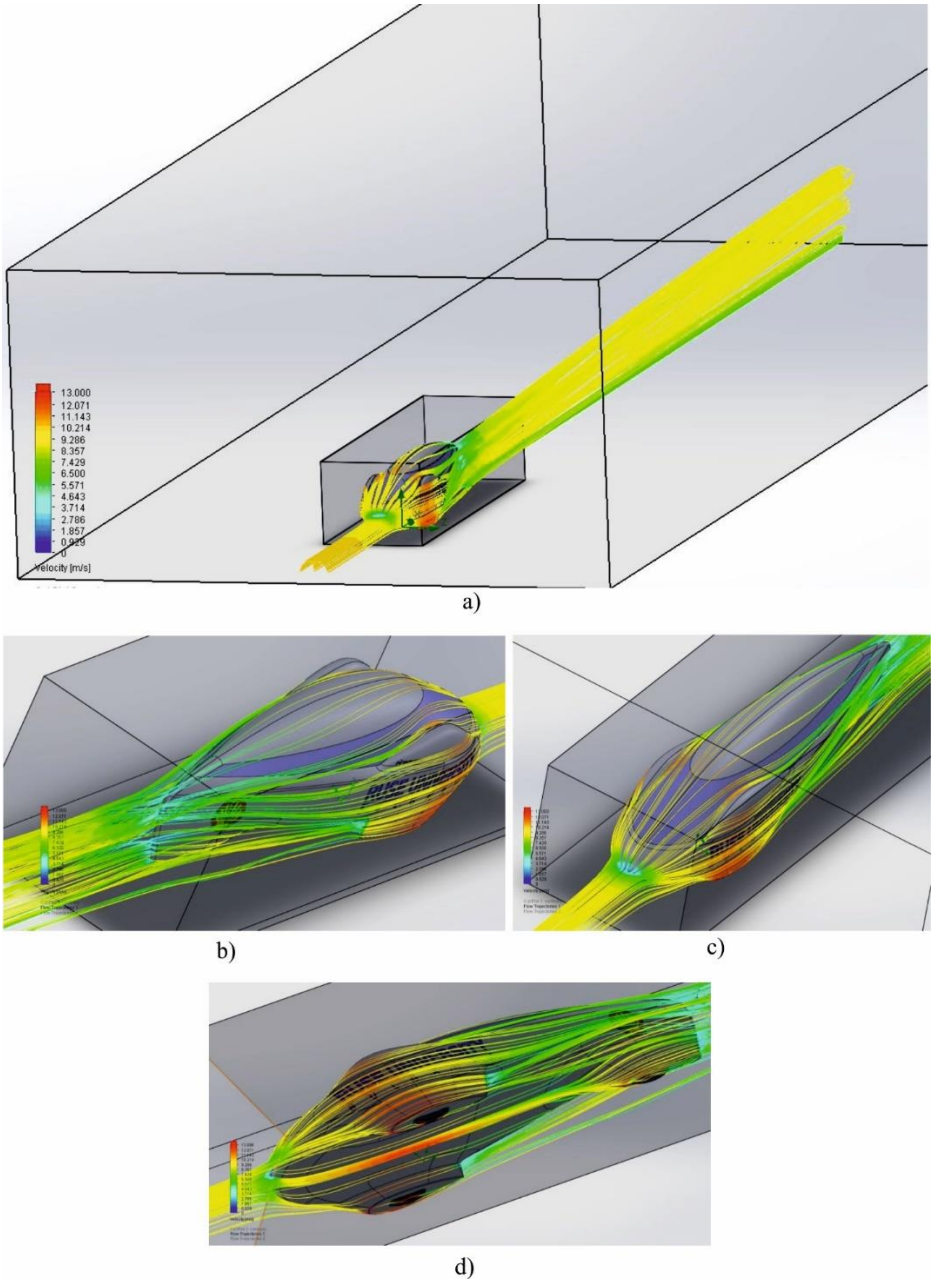

Fig. 8. The Current lines (trajectories) stained by isotahs

The velocity field forms the pressure field. The isobars of the flow space are not considered. It is more important to have an isobar's image on the surface of the vehicle (Fig. 9). There are three zones - front and rear with high pressure values in the range $101315\ to\ 101335\ Pa$ and a median with a pressure $101280\ to\ 101305\ Pa$, that surrounds the belt between the front and rear wheels.

The pressure differential between the front and rear zones forms the aerodynamic resistance of the vehicle's shape, while in the middle zone the aerodynamic resistance of viscous friction on the walls is formed. This is evident from (Fig. 10) where the intensity of the vortices is presented. The intensity of the vortices arises from the gradient of the velocity of the current near the walls of the vehicle. The area with the highest intensity of the vortex is coloured red and covers the back and down end of the vehicle, varying in the range $\omega = 140\ to\ 170\ s^{-1}$.

The fields of pressure and intensity of vortices on the surface of the vehicle form the force interaction of the flow with the vehicle, respectively the power indicators - the force of the drag and the lift force. The information about these fields allows you to optimize its shape.

Another method of imaging the current used in the report is with the current lines (trajectories) shown in Fig. 8. Before and after the vehicle, they are parallel to each other, and along the vehicle they do not tear off its sides. This means that the shape of the vehicle as a whole and the elements of its body (the fenders) are not the cause of whirls.

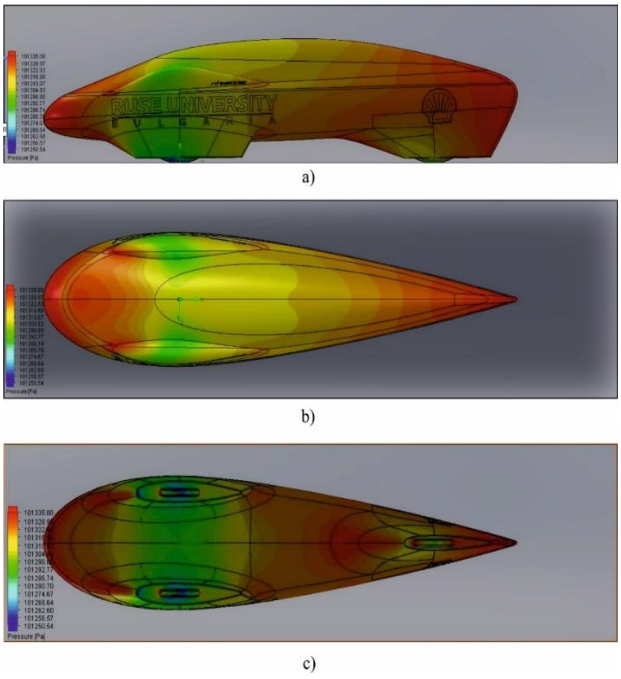

Fig. 9. Picture on the left, top, and bottom surfaces of the vehicle

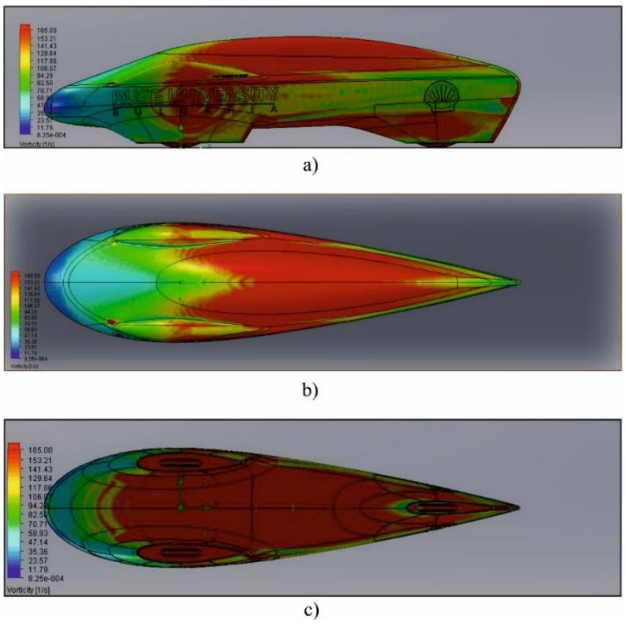

Fig. 10. Intensity of vortices

The distribution of velocity and pressure along the length of control lines (Fig. 4b) and (Fig. 4c) as mentioned above can serve as a benchmark between different methods (theoretical, computational, experimental) for study. This can also be used to determine the thickness of the boundary layer along the walls of the vehicle, and then calculate the transverse gradient of velocity, which is an indicator for the intensity of the viscous friction. The results of the digital survey show that the thickness of the boundary layer along the circumference of the section with the X-Y plane changes in the interval $\delta_i = 0{,}01\ to\ 0{,}025\ m$ and the gradient of the velocity $\Delta v/\Delta y_i = 400\ to\ 1000\ s^{-1}$.

The results of the calculations in the form of force-velocity characteristics of the drag force X and the lift force Y in relation to the vehicle speed are shown in (Fig. 11). When the speed of the vehicle is varied within the range $v_i = 2\ to\ 10\ m/s$, the drag forces are $X = 0{,}12\ to\ 1{,}26\ N$, and for the lift force Y$= -0{,}07\ to\ 3{,}6\ N$. The lift force has negative values, that is, together with the weight force, presses the vehicle to the road.

Their respective aerodynamic characteristics were also obtained, $C_x = f(R_e)$ and $C_y = f(R_e)$ show on (Fig. 12). When the Reynolds number is varied within the range $R_e = 80000\ to\ 400000$, the values of the drag force coefficient are $C_x = 0{,}095\ to\ 0{,}065$, and of the lifting force coefficient $C_y = 0{,}051\ to\ 0{,}186$.

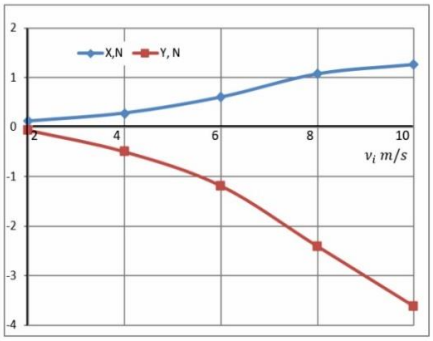

Fig. 11. Speed characteristics obtained by numerical simulation of the flow.

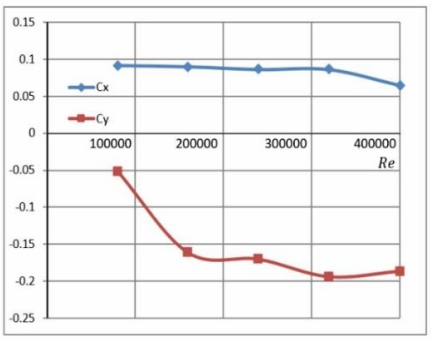

Fig. 12. Aerodynamic characteristics $C_x = f(R_e)$ and $C_y = f(R_e)$ obtained by numerical simulation.

The characteristic aerodynamic losses of power-velocity (Figure 13) is quadratic. When the vehicle speed changes within the range e $v = 2\ to\ 10\ m/s$, the power losses increase within the range $P = 0{,}18\ to\ 12{,}7\ W$.

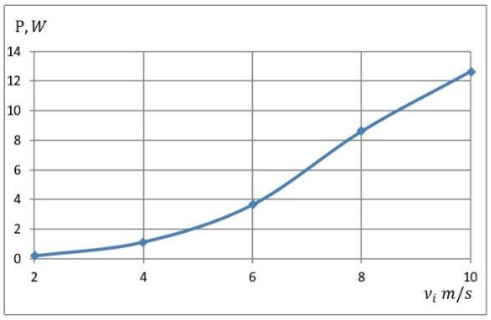

Fig. 13. Characteristic aerodynamic losses of power-speed

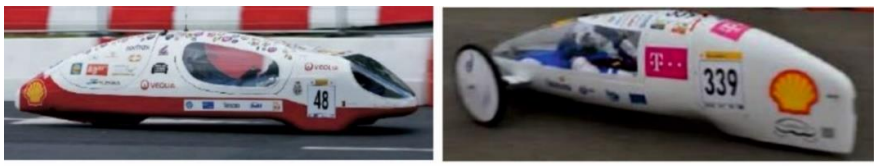

Fig. 14. Vehicle models involved in Shell Eco-marathon competition [7], [8]

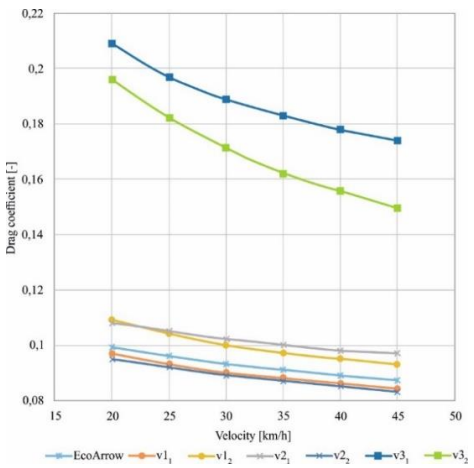

Fig. 15. Aerodynamic characteristics for vehicles participating in the Shell Eco-marathon [7], [8]

In the (Fig. 14) are given models of some vehicles that participated in the Shell Eco-marathon race, and in (Fig. 15), their respective aerodynamic characteristics. This report is used to compare the aerodynamic characteristics of a research vehicle constructed and manufactured in Rousse University [9] with the characteristics of vehicles which have taken part in competition Shell Eco-Marathon. If the characteristic of the vehicle $C_x = f(v)$ is drawn in (Fig. 15), it will be under all others.

4. Conclusions

From the comparison of the aerodynamic characteristics of the University of Ruse vehicle (Team Avtomobilist) (Figure 12) and the aerodynamic characteristics of the vehicles that participated in the Shell Eco-marathon race (Figure 15), could be seen that they have the qualities and quantities corresponding, but the aerodynamic characteristics of the Team Avtomobilist's vehicle are, better. At vehicle speed $v = 10\ m/s$, the smallest value of the drag coefficient of the vehicles involved in the race is $C_x = 0{,}085$, whereas the one of the Team Avtomobilist is $C_x = 0{,}065$, i.e. with 25% smaller.

The weight of the vehicle along with the weight of the pilot is $G_\Sigma = 1000\ N$. The lift force at the speed of movement $v = 10\ m/s$ coincides with the direction of the force of the weight, and its value is $Y = -3{,}6\ N$ (Fig. 11), i.e. $0{,}36\ \%$ from G_Σ. It means, that it is negligible. The approximation of aerodynamic characteristics by form and values is considered as a verification of the numerical model obtained by simulation with the Flow Simulation CFD program. The main source of the external air flow disturbance is the shape of the fenders (Fig. 7a). To reduce aerodynamic drag, the shape can be optimized. The maximum power of the electric motor is $P_{max} = 200\ W$, while the aerodynamic power losses at the speed $v = 10\ m/s$ of the vehicle are $\Delta P = 12{,}7\ W$ (Fig. 15). Therefore, 6.35% of the power of the electric motor is spent to overcome aerodynamic resistances. The remaining power losses of 93.65% are in the electric motor and the transmission. Future research should focus on improving the aerodynamic channel for best calibration of CFD model.

5. Acknowledgments

The present document has been produced with the financial assistance of the Project 2018-RU-07 "Creation of a complex mobile laboratory platform for research and approbation of environmentally friendly technical solutions".

6. References

[1] Oliveria Santos, R., Lyra, P. R. M., Araujo Souza, M. R., Souza Junior, M. A. (2012). Aerodynamic Design of Super Efficient Vehicle, SAE International.

[2] Ahmed, H. & Chacko, S. (2012) Computational Optimization of Vehicle Aerodynamics, Annals of DAAAM for 2012 & Proceedings of the 23rd International DAAAM Symposium, Volume 23, No.1.

[3] Antonova, D. & Stoycheva, B. (2018). Approved model of factors, influencing the management process in developing new products. In: The 6th International Conference Innovation Management, Entrepreneurship and Sustainability (IMES 2018), Czech Republic, Vysoká škola ekonomická v Praze, Nakladatelství Oeconomica – Praha, 2018, Nakladatelství Oeconomica, pp. 38-54.

[4] Kunev, S., Kostadinova, I. & Stoycheva, B. (2017). Business Governance and Corporate Social Responsibility in Bulgaria// Annals of „Eftimie Murgu", University Reşiţa, Fascicle II. Economic Studies, No XXIV, pp. 99-115,

[5] Terziev A. (2014). Specifics in numerical modelling of flow past a square-cylinder, Proceedings of University of Ruse, volume 53, book 1.2, pp. 143-148.

[6] Tuzharov, K., Popov, G., Zeleva, I., Klimentov, K., Nikolaev. N., Kostov, B., Ahmedov, A. (2015). Theoretical study of a tachometric flowmeter with CFD product Flow Simulation, Proceedings of University of Ruse, volume 46, book 1, pp. 273-279.

[7] Danec. W. (2014). Determination of the drag coefficient high performance electric vehicle, Modelovanie inzinierskie, N 52, ISSN 1896-771X.

[8] Cieslinski, A. (2016) Investigations of aerodynamic of super effective vehicle for drag reduction. Mechanics and mechanical engeneering, vol. 20, N3, 2016, 295-308, Lodz university of technology.

[9] Iliev, S., Gunev D., Dobrev V. (2017). Improving engineering education through the design and manufacture of electric car for the Shell Eco-marathon competition, ERS Spectrum (Educational Research Service), Vol. 29, No. 2, ISSN: 0740-7874